

A relativistic quark model for the Ω^- electromagnetic form factors

G. Ramalho^{1,2}, K. Tsushima³ and Franz Gross^{1,4}

¹Thomas Jefferson National Accelerator Facility, Newport News, VA 23606, USA

²Centro de Física Teórica de Partículas, Ave. Rovisco Pais, 1049-001 Lisboa, Portugal

³EBAC in Theory Center, Thomas Jefferson National Accelerator Facility, Newport News, VA 23606, USA and

⁴College of William and Mary, Williamsburg, VA 23185, USA

(Dated: October 30, 2018)

We compute the Ω^- electromagnetic form factors and the decuplet baryon magnetic moments using a quark model application of the Covariant Spectator Theory. Our predictions for the Ω^- electromagnetic form factors can be tested in the future by lattice QCD simulations at the physical strange quark mass.

I. INTRODUCTION

The Ω^- baryon has a unique position in the baryon decuplet. A naive SU(6) quark model describes Ω^- as a state with three strange quarks in a totally symmetric flavor-spin-space, e.g.

$$|\Omega^-; S = \frac{3}{2}, S_z = +\frac{3}{2}\rangle = |s\uparrow s\uparrow s\uparrow\rangle. \quad (1)$$

As the strange quark decays via the weak interaction, the Ω^- has an extremely long lifetime ($\tau \simeq 8 \times 10^{-11}$ s) compared to the other decuplet members which have at least one light quark. Because of this, the world's average of the measurements of the magnetic dipole moment has a high precision, $\mu_{\Omega^-} = (-2.02 \pm 0.05)\mu_N$ [1], with μ_N the nuclear magneton.

Long before its experimental determination, the Ω^- magnetic moment was estimated using a SU(6) symmetric quark model [2], which gave $\mu_{\Omega^-} = -\mu_p = -2.79\mu_N$ (where μ_p is the proton magnetic moment in units of nuclear magneton). That model was improved considering the individual contributions of the quark magnetic moments and the SU(3) symmetry breaking (naive or static quark model) leading to $\mu_{\Omega^-} \simeq -1.8\mu_N$ [3, 4]. The naive result was then corrected including non-static corrections, sea quark contributions, quark orbital momentum effects, relativistic effects and others, using several formalisms [5, 6, 7, 8, 9, 10, 11, 12]. In 1991 the Ω^- magnetic moment was measured at Fermilab [13]. The result was $\mu_{\Omega^-} = (-1.94 \pm 0.22)\mu_N$. The most recent measurement is from 1995 and gives $\mu_{\Omega^-} = (-2.024 \pm 0.056)\mu_N$ [14]. The combination of the two results leads to $\mu_{\Omega^-} = (-2.019 \pm 0.054)\mu_N$ [1, 14]. Several works followed with estimations of μ_{Ω^-} [15, 16, 17, 18, 19, 20, 21, 22, 23, 24, 25, 26, 27, 28, 29]. The Ω^- electric quadrupole moment was also predicted [22, 23, 30, 31, 32, 33, 34, 35, 36, 37, 38, 39, 40], although there is no experimental result. Several works estimate the Ω^- electromagnetic radius [11, 15, 21, 22, 37, 38, 39, 41]. Also the Ω^- magnetic octupole moment was been estimated [30, 40, 42].

The magnetic moment [43, 44, 45, 46] and the Ω^- form factors [44, 47] (including the electric quadrupole

and magnetic dipole moments) have also been calculated using lattice QCD. The study of the Ω^- mass in lattice QCD is nowadays an important topic of investigation helping to constrain the (physical) strange quark mass in the quenched and dynamical calculations [48, 49, 50, 51].

In this work we extend the quark model based on the Covariant Spectator Theory [52, 53], originally developed to describe the nucleon form factors and properties of the Δ , to the full decuplet of baryons containing strange quarks. In the previous work this spectator formalism was applied to the $\gamma N \rightarrow \Delta$ transition form factors [54, 55, 56] as well as the nucleon [57] and Δ [58, 59] electromagnetic form factors. The flavor-spin structure of the Ω^- is very similar to that of the Δ . One gets the Ω^- either by replacing the u quarks by the s quarks in the Δ^{++} , or replacing the d quarks by the s quarks in the Δ^- .

However, the Δ is significantly more unstable ($\tau_{\Delta} \simeq 6 \times 10^{-24}$ s) than Ω^- , and this makes it very hard to measure the Δ electromagnetic form factors experimentally. At present, to compare with theoretical predictions, we usually have to rely on the pseudo-data, namely those extracted from lattice QCD. Even then one must be careful, since the lattice QCD results are obtained with unphysical pion masses (heavy quark masses) which induce extra ambiguities, as discussed in Refs. [58, 59]. On the other hand, the situation for the Ω^- is completely different. It is presently possible to extract the magnetic dipole moment [45, 46] and the electric and magnetic dipole form factors [47] in lattice QCD with the physical strange quark mass of $m_s \approx 100$ MeV. Thus, theoretical predictions of the Q^2 dependence for the Ω^- electromagnetic form factors can be directly compared with the lattice QCD data.

II. SPECTATOR QUARK MODEL

The covariant spectator quark model that we are using (developed in Refs. [54, 55, 57] for the SU(2) light quark sector) describes spin 1/2 and 3/2 three-quark systems

as states of an off-shell quark and an on-shell spectator diquark [57, 60]. The diquark is intended to be a simple representation of the two *noninteracting* on-shell spectator quarks, with a mass that varies from $4m_q^2$ to infinity (m_q is the quark mass). To simplify the calculation while still preserving the important physics, the integral over this mass is evaluated at some mean value m_D (this mass was previously denoted m_s , but in this work m_s will be reserved for the strange quark mass), which becomes a parameter of the model. As it turns out, this parameter scales out of all form factor integrals, so that the results are independent of it and it does not enter into the fits [54, 57]. The vertex functions are symmetrized so that (in the relativistic impulse approximation) all form factors and transition amplitudes become a sum over terms in which the photon couples to each flavor of (off-shell) quark in turn with the other two (on-shell) quarks composing the on-shell diquark. In this way interactions with *all* of the quarks are counted without including couplings to the diquark (in fact, to include them would be to over count). Finally, our quarks are *constituent* quarks, with a form factor of their own, modeled using vector meson dominance.

A decuplet baryon (B) with a spin 3/2 wave function based on this quark-diquark model with a pure orbital S-state can be generically written [54, 55]:

$$\begin{aligned} \Psi'_B(P, k; \lambda, \lambda_B) &= -\psi_B(P, k) |B\rangle \varepsilon_P^{\alpha*}(\lambda) u_\alpha(P; \lambda_B) \\ &= \Psi_B(P, k) |B\rangle, \end{aligned} \quad (2)$$

where Ψ_B (which suppresses the polarizations λ and λ_B and extracts $|B\rangle$) is a shorthand notation we will use through this paper. Here P (k) is the baryon (diquark) momentum, $\lambda = 0, \pm 1$ the diquark polarization, $\lambda_B = 0, \pm 1/2, \pm 3/2$ the baryon spin projection, u_α the Rarita-Schwinger vector spinor, $\varepsilon_P^{\alpha*}$ the polarization state of the outgoing diquark, and $|B\rangle$ is a flavor state which will be specified latter. As for $\psi_B(P, k)$, it is a *real scalar function* that models the momentum distribution of the quark-diquark system. For the diquark polarization states we adopt the fixed-axis basis [53], where the diquark spin states are characterized by the momentum of the baryon P , instead of the diquark momentum k . Although this choice might be unconventional, it generalizes the non relativistic structure for both the spin 1/2 and spin 3/2 cases [54, 57]. In addition, the wave function $\Psi_B(P, k)$ satisfies the equation $(M_B - \not{P})\Psi_B = 0$, where M_B is the baryon mass [53, 54, 55, 57].¹ Eq. (2) is the flavor generalization of the Δ S-state wave function we have used successfully in the past [54, 58]. In this work we assume that the decuplet baryons can be approximated as a quark-diquark in a spatial S-wave state. Although there is strong evidence for the presence of D-states in

the Δ , the D-states admixtures are small [56], and the dominant form factors, such as the electric charge and magnetic dipole moment, can be well described without the D-state components [58, 59, 61].

A. Electromagnetic current

The electromagnetic current of the baryon in a elastic process can be written in the covariant spectator quark model [54, 55, 57, 59]:

$$J_B^\mu(q) = \sum_{a=1}^3 \sum_{\lambda} \int_{k_a} \bar{\Psi}'_B(P_+, k_a) j_a^\mu(q) \Psi'_B(P_-, k_a), \quad (3)$$

where P_- (P_+) is the initial (final) baryon momentum, k_a the momentum of the a -th diquark (the companion to the a -th quark, which has momentum $P - k_a$), and $q = P_+ - P_-$. As for j_a^μ it represents the a -th quark current operator. Note that Eq. (3) corresponds to an impulse approximation in which the electromagnetic interaction is described as a sum over terms in which the photon couples to *each* of the three quarks in turn. The integral sign \int_k is a short-hand notation for

$$\int_k \equiv \int \frac{d^3k}{(2\pi)^3 (2E_D)}, \quad (4)$$

the covariant integration volume, where $E_D = \sqrt{m_D^2 + k^2}$ is the energy of the on-mass-shell diquark with mass m_D . The sum over a includes the interactions with all three quarks included in the $|B\rangle$ state (as described further below), but since the wave function must be exactly symmetric in spin-flavor-coordinate space, each of the three terms in the sum is exactly identical, so that the current matrix element is simply

$$J_B^\mu(q) = 3 \sum_{\lambda} \int_k \bar{\Psi}_B(P_+, k) \langle B | j^\mu(q) | B \rangle \Psi_B(P_-, k), \quad (5)$$

where, for definiteness, we take $k = k_3$ to be four-momentum of the third diquark (but the choice does not matter).

The quark electromagnetic current can be expressed in terms of a Dirac j_1 and a Pauli j_2 form factors [54, 57]:

$$j^\mu(q) = j_1(Q^2) \gamma^\mu + j_2(Q^2) \frac{i\sigma^{\mu\nu} q_\nu}{2M_N}, \quad (6)$$

where M_N is the nucleon mass, and $Q^2 = -q^2$. The Dirac and Pauli form factors j_i ($i = 1, 2$) are diagonal operators in the 3×3 flavor space which can be written,

$$j_i(Q^2) = \frac{1}{6} f_{i+}(Q^2) \lambda_0 + \frac{1}{2} f_{i-}(Q^2) \lambda_3 + \frac{1}{6} f_{i0}(Q^2) \lambda_s, \quad (7)$$

where $f_{in}(Q^2)$, with $n = \pm, 0$, represents respectively the isoscalar (+), isovector (−) and s quark (0) form factors,

¹ The Fixed-Axis polarization basis also has the advantage of allowing a complete identification of the angular momentum components of the wave function. See Refs. [54, 55] for details.

B	$ B\rangle$	$\overline{j_{iB}}$
Δ^-	$ddd = 1, -1, 0\rangle_D d\rangle$	$\frac{1}{2}[f_{i+} - 3f_{i-}]$
Δ^0	$\frac{1}{\sqrt{3}}[ddu + dud + udd] = \sqrt{\frac{2}{3}}\left\{ 1, -1, 0\rangle_D u\rangle + \frac{1}{\sqrt{2}} 1, 0, 0\rangle_D d\rangle\right\}$	$\frac{1}{2}[f_{i+} - f_{i-}]$
Δ^+	$\frac{1}{\sqrt{3}}[uud + udu + duu] = \sqrt{\frac{2}{3}}\left\{ 1, 1, 0\rangle_D d\rangle + \frac{1}{\sqrt{2}} 1, 0, 0\rangle_D u\rangle\right\}$	$\frac{1}{2}[3f_{i+} - f_{i-}]$
Δ^{++}	$uuu = 1, 1, 0\rangle_D u\rangle$	$\frac{1}{2}[f_{i+} + 3f_{i-}]$
Σ^{*-}	$\frac{1}{\sqrt{3}}[dds + dsd + sdd] = \sqrt{\frac{2}{3}}\left\{\frac{1}{\sqrt{2}} 1, -1, 0\rangle_D s\rangle + \left \frac{1}{2}, -\frac{1}{2}, -1\right\rangle_D d\rangle\right\}$	$\frac{1}{3}[f_{i+} - 3f_{i-} - f_{i0}]$
Σ^{*0}	$\frac{1}{\sqrt{6}}[uds + dus + usd + sud + dsu + sdu] = \frac{1}{\sqrt{3}}\left\{ 1, 0, 0\rangle_D s\rangle + \left \frac{1}{2}, \frac{1}{2}, -1\right\rangle_D d\rangle + \left \frac{1}{2}, -\frac{1}{2}, -1\right\rangle_D u\rangle\right\}$	$\frac{1}{3}[f_{i+} - f_{i0}]$
Σ^{*+}	$\frac{1}{\sqrt{3}}[uus + usu + suu] = \sqrt{\frac{2}{3}}\left\{\frac{1}{\sqrt{2}} 1, 1, 0\rangle_D s\rangle + \left \frac{1}{2}, \frac{1}{2}, -1\right\rangle_D u\rangle\right\}$	$\frac{1}{3}[f_{i+} + 3f_{i-} - f_{i0}]$
Ξ^{*-}	$\frac{1}{\sqrt{3}}[dss + sds + ssd] = \sqrt{\frac{2}{3}}\left\{\left \frac{1}{2}, -\frac{1}{2}, -1\right\rangle_D s\rangle + \frac{1}{\sqrt{2}} 0, 0, -2\rangle_D d\rangle\right\}$	$\frac{1}{6}[f_{i+} - 3f_{i-} - 4f_{i0}]$
Ξ^{*0}	$\frac{1}{\sqrt{3}}[uss + sus + ssu] = \sqrt{\frac{2}{3}}\left\{\left \frac{1}{2}, \frac{1}{2}, -1\right\rangle_D s\rangle + \frac{1}{\sqrt{2}} 0, 0, -2\rangle_D u\rangle\right\}$	$\frac{1}{6}[f_{i+} + 3f_{i-} - 4f_{i0}]$
Ω^-	$ sss\rangle = 0, 0, -2\rangle_D s\rangle$	$-f_{i0}$

TABLE I: Flavor wave functions $|B\rangle$ expressed both in terms of their three-quark content and their quark-diquark content, using the diquark notation of Table II. The right column gives $\overline{j_{iB}}$. One gets the contribution of the electric charge function \tilde{e}_B for $i = 1$, while for $i = 2$ one gets the contribution of the anomalous magnetic moment function $\tilde{\kappa}_B$.

$ I, I_z, S\rangle_D$	$ q_1 q_2\rangle$
$ 1, 1, 0\rangle_D$	$ uu\rangle$
$ 1, 0, 0\rangle_D$	$\frac{1}{\sqrt{2}}\{ ud\rangle + du\rangle\}$
$ 1, -1, 0\rangle_D$	$ dd\rangle$
$\left \frac{1}{2}, \frac{1}{2}, -1\right\rangle_D$	$\frac{1}{\sqrt{2}}\{ us\rangle + su\rangle\}$
$\left \frac{1}{2}, -\frac{1}{2}, -1\right\rangle_D$	$\frac{1}{\sqrt{2}}\{ ds\rangle + sd\rangle\}$
$ 0, 0, -2\rangle_D$	$ ss\rangle$

TABLE II: Diquark wave functions, with I and I_z the diquark isospin and its z projection, and S the diquark strangeness.

and λ_0 , λ_3 , and λ_s are the diagonal matrices

$$\lambda_0 = \begin{pmatrix} 1 & 0 & 0 \\ 0 & 1 & 0 \\ 0 & 0 & 0 \end{pmatrix}, \quad \lambda_3 = \begin{pmatrix} 1 & 0 & 0 \\ 0 & -1 & 0 \\ 0 & 0 & 0 \end{pmatrix}, \quad (8)$$

$$\lambda_s \equiv \begin{pmatrix} 0 & 0 & 0 \\ 0 & 0 & 0 \\ 0 & 0 & -2 \end{pmatrix}, \quad (9)$$

that act on the quark wave function in flavor space

$$q = \begin{pmatrix} u \\ d \\ s \end{pmatrix}. \quad (10)$$

Using the normalization $f_{1n}(0) = 1$, we recover the usual

relation for the quark charge:

$$j_1(0) = \frac{1}{2}\lambda_3 + \frac{1}{2\sqrt{3}}\lambda_s, \quad (11)$$

with $\lambda_8 = \frac{1}{\sqrt{3}}[\lambda_0 + \lambda_s]$, the SU(3) generator. Equation (7) generalizes the current in Refs. [54, 57] to include s quarks. In Ref. [57], $f_{2\pm}(Q^2)$ was normalized to $f_{2\pm}(0) = \kappa_{\pm}$ in order to reproduce the nucleon magnetic moments, μ_p and μ_n . This fixes the values, $\kappa_+ = 1.639$ and $\kappa_- = 1.825$. The extension of this strange quarks gives $e_s \kappa_s = \frac{1}{6}f_{20}(0)\lambda_s$ which leads to the normalization $f_{20}(0) = \kappa_s$.

B. Computing the flavor matrix elements of the current

The flavor wave functions for the baryons in the decuplet are given in Table I. They can be expressed in two ways: first, as a direct product of the flavor states of the three quarks, suitably symmetrized, or second, as a sum over direct products of a diquark state described by isospin, I , z projection of the isospin, I_z , and strangeness, S , times the appropriate flavor of quark number 3. For example, the flavor wave function of the Σ^{*0} , the completely symmetric uds (in this notation, particle 1 is a u quark, particle 2 a d quark, and particle 3 an s quark) can be written in two equivalent forms

$$\begin{aligned} |\Sigma^{*0}\rangle &= \frac{1}{\sqrt{6}}[(du + ud)s + (ds + sd)u + (us + su)d] \\ &= \frac{1}{\sqrt{3}}\left\{|1, 0, 0\rangle_D |s\rangle + \left|\frac{1}{2}, -\frac{1}{2}, -1\right\rangle_D |u\rangle \right. \\ &\quad \left. + \left|\frac{1}{2}, \frac{1}{2}, -1\right\rangle_D |d\rangle\right\}, \end{aligned} \quad (12)$$

where the diquark states are defined in Table II. In the second line of Eq. (12) we have written the state as a sum of terms with particles 1 and 2 treated as a diquark, and particle 3 as a single quark. At this stage these two representations are completely equivalent, but later, when we convert these states to the covariant quark-diquark model, we allow quark 3 to be off-shell, and treat the diquark pair as a single particle of mass m_D , as described above. This will break the symmetry between the three quarks, which is then restored by symmetrizing the state again. When the electromagnetic matrix elements are calculated, these separate off-shell pieces do not interfere with each other, and the total matrix element is simply three times the matrix element with particle 3 off-shell (as discussed above).

Using these flavor wave functions we compute the flavor matrix elements of the current

$$\overline{j}_{iB} = 3\langle B|j_i(3)|B\rangle, \quad i = \{1, 2\} \quad (13)$$

where $|B\rangle$ is the flavor wave functions described above, and we have incorporated the factor of 3 from Eq. (5) into the definition of \overline{j}_{iB} . Using (13), the current (5) becomes

$$J_B^\mu(q) = \sum_\lambda \int_k \overline{\Psi}_B(P_+, k) \times \left[\overline{j}_{1B} \gamma^\mu + \overline{j}_{2B} \frac{i\sigma^{\mu\nu} q_\nu}{2M_N} \right] \Psi_B(P_-, k). \quad (14)$$

To calculate the matrix elements \overline{j}_{iB} we use the flavor wave functions from Table I. As an example, let us calculate \overline{j}_{iB} for Σ^{*0} state. Using the quark-diquark representation with the notation $B = \Sigma^{*0}$, and recalling that all of the diquark wave functions are orthonormal, we obtain three identical terms

$$\begin{aligned} \overline{j}_{i\Sigma^{*0}} &= 3\langle \Sigma^{*0} | \{ \frac{1}{6}f_{i+}\lambda_0 + \frac{1}{2}f_{i-}\lambda_3 + \frac{1}{6}f_{i0}\lambda_s \} | \Sigma^{*0} \rangle \\ &= \langle s | \{ \frac{1}{6}f_{i+}\lambda_0 + \frac{1}{2}f_{i-}\lambda_3 + \frac{1}{6}f_{i0}\lambda_s \} | s \rangle \\ &\quad + \langle d | \{ \frac{1}{6}f_{i+}\lambda_0 + \frac{1}{2}f_{i-}\lambda_3 + \frac{1}{6}f_{i0}\lambda_s \} | d \rangle \\ &\quad + \langle u | \{ \frac{1}{6}f_{i+}\lambda_0 + \frac{1}{2}f_{i-}\lambda_3 + \frac{1}{6}f_{i0}\lambda_s \} | u \rangle \\ &= -\frac{1}{3}f_{i0} + (\frac{1}{6}f_{i+} - \frac{1}{2}f_{i-}) + (\frac{1}{6}f_{i+} + \frac{1}{2}f_{i-}) \\ &= \frac{1}{3}f_{i+} - \frac{1}{3}f_{i0}, \end{aligned} \quad (15)$$

where the diquark states appear in the second to forth lines only as a normalization factor of unity. All of the matrix elements, calculated in the same manner, are given in the third column of Table I.

Similarly, we can evaluate the electric charge \tilde{e}_B and anomalous magnetic moment $\tilde{\kappa}_B$ quark form factors defined by

$$\tilde{e}_B(Q^2) = \overline{j}_{1B}(Q^2), \quad \tilde{\kappa}_B(Q^2) = \overline{j}_{2B}(Q^2). \quad (16)$$

In the limit $Q^2 = 0$ the form factors give the electric charge e_B and anomalous magnetic moment κ_B .

III. BARYON FORM FACTORS

The spin 3/2 baryon (B) electromagnetic form factors, $F_i^*(Q^2)$ ($i = 1, \dots, 4$), are defined by the current [58, 62, 63]:

$$J_B^\mu = -\bar{u}_\alpha \left\{ \left[F_1^* g^{\alpha\beta} + F_3^* \frac{q^\alpha q^\beta}{4M_B^2} \right] \gamma^\mu \right\} u_\beta - \bar{u}_\alpha \left\{ \left[F_2^* g^{\alpha\beta} + F_4^* \frac{q^\alpha q^\beta}{4M_B^2} \right] \frac{i\sigma^{\mu\nu} q_\nu}{2M_B} \right\} u_\beta. \quad (17)$$

Using the wave function (2), the hadronic current (5) defined by the model, and the generic structure of Eq. (17), we can write the form factors $F_i^*(Q^2)$ in terms of the charge \tilde{e}_B and anomalous magnetic moment $\tilde{\kappa}_B$ form factors defined in Eq. (16). Using the multipole form factors given by a linear combination of F_i^* [58, 62, 63], we get the expressions for the electric charge and magnetic dipole form factors,

$$G_{E0}(Q^2) = \left(\tilde{e}_B(Q^2) - \tau \frac{M_B}{M_N} \tilde{\kappa}_B(Q^2) \right) \mathcal{I}_B(Q^2), \quad (18)$$

$$G_{M1}(Q^2) = \left(\tilde{e}_B(Q^2) + \frac{M_B}{M_N} \tilde{\kappa}_B(Q^2) \right) \mathcal{I}_B(Q^2), \quad (19)$$

where $\tau = \frac{Q^2}{4M_B^2}$. Note that the $Q^2 = 0$ limit of these form factors defines the charge [$e_B = G_{E0}(0)$] and magnetic dipole moment [$\mu_B = G_{M1}(0) \frac{e}{2M_B}$]. The factor \mathcal{I}_B is the overlap integral between the initial and final scalar part of the wave function in Eq. (2),

$$\mathcal{I}_B(Q^2) = \int_k \psi_B(P_+, k) \psi_B(P_-, k), \quad (20)$$

and is real. In the limit $Q^2 = 0$, charge conservation requires $\mathcal{I}_B(0) = 1$.

The derivation of Eqs. (18) and (19) is given in Ref. [58] for the Δ case in the same S-state approximation. The remaining form factors are G_{E2} and G_{M3} . In the S-state approximation, G_{E2} and G_{M3} vanish [58]. The differences between Eqs. (18)-(19) and the corresponding expressions in Ref. [58] are the baryon mass M_B (which replaces M_Δ) and \tilde{e}_B and $\tilde{\kappa}_B$ (which replace \tilde{e}_Δ and $\tilde{\kappa}_\Delta$). Note that the mass ratio, $\frac{M_B}{M_N}$, results from the simplification of the Pauli current contribution of Eq. (6), possible because the states satisfy the Dirac equation, $(M_B - \not{P})u_\alpha(P, \lambda_B) = 0$ [54, 55, 58].

A. Baryon decuplet magnetic moments

The $Q^2 = 0$ limit of G_{M1} gives the baryon magnetic dipole moment μ_B in units of $\frac{e}{2M_B}$. Converting the result into nuclear magnetons μ_N gives

$$\mu_B = G_{M1}(0) \frac{M_N}{M_B} \mu_N, \quad (21)$$

or

$$\mu_B = \left(e_B + \frac{M_B}{M_N} \kappa_B \right) \frac{M_N}{M_B} \mu_N. \quad (22)$$

Recalling that $\kappa_B = \overline{j_{2B}}(0)$ and using the formulae for $\overline{j_{2B}}$ from the third column of Table I with $f_{2+}(0) = \kappa_+ = 2\kappa_u - \kappa_d$ and $f_{2-}(0) = \kappa_- = \frac{2}{3}\kappa_u + \frac{1}{3}\kappa_d$, the decuplet magnetic moments can be expressed in terms of the anomalous moments of the three quarks (and their charges), as listed in table III. If we ignore some pion cloud effects (discussed further below), the anomalous moments of the u and d quarks can be determined by a fit to the neutron and proton magnetic moments [57], giving $\kappa_u = 1.778$ and $\kappa_d = 1.915$. These values lead to the predictions [58]: $\mu_{\Delta^{++}} = 5.11\mu_N$, $\mu_{\Delta^+} = 2.51\mu_N$, $\mu_{\Delta^0} = -0.09\mu_N$ and $\mu_{\Delta^-} = -2.70\mu_N$. For the other members of the decuplet results are dependent on the strange quark anomalous magnetic moment, κ_s , to be determined next.

B. Ω^- magnetic moment

For the Ω^- with $e_B = -1$ and $\kappa_B = -\kappa_s$ one gets

$$\mu_{\Omega^-} = - \left(1 + \frac{M_\Omega}{M_N} \kappa_s \right) \frac{M_N}{M_\Omega} \mu_N. \quad (23)$$

For a simple estimate of μ_{Ω^-} we use $\kappa_s = \frac{1}{2}(\kappa_u + \kappa_d)$ corresponding to an approximate SU(3) limit, since SU(2) is already broken ($\kappa_u \neq \kappa_d$). This estimate, which we denote by SU'(3), gives $\mu_{\Omega^-} = -2.41\mu_N$, where the experimental value is $\mu_{\Omega^-} = (-2.02 \pm 0.05)\mu_N$, which deviates by about 20%. The results for Σ^* and Ξ^* magnetic moments in the SU'(3) approximation are also given in table III together with the nonrelativistic naive SU(6) quark model (NRQM) values [3, 4].

Unfortunately there is no experimental data for the other members of the decuplet aside from the Δ (with no strange quarks). Under these circumstances the experimental value for μ_{Ω^-} is the only physical constraint available to fix κ_s . Following the procedure used in Ref. [57] where κ_u and κ_d were constrained to fit the nuclear magnetic moments (μ_p and μ_n), we use Eq. (23) and adjust κ_s to fit the Ω^- magnetic moment exactly. This fixes $\kappa_s = 1.462$.

Once κ_s is fixed, we can make predictions for all the strange decuplet baryon magnetic moments. The results are presented in Table III with the label CST for the quark model based on the Covariant Spectator Theory.

IV. MODEL FOR THE s QUARK CURRENT AND WAVE FUNCTIONS

In previous work [54, 55, 57] the quark form factors were defined in the SU(2) sector (u, d) by using a

B	κ_B	NRQM	SU'(3)	CST
Σ^{*-}	$-\frac{1}{3}[2\kappa_d + \kappa_s]$	-2.47	-2.57	-2.44
Σ^{*0}	$\frac{1}{3}[2\kappa_u - \kappa_d - \kappa_s]$	0.32	-0.07	0.06
Σ^{*+}	$\frac{1}{3}[4\kappa_u - \kappa_s]$	3.11	2.43	2.56
Ξ^{*-}	$-\frac{1}{3}[\kappa_d + 2\kappa_s]$	-2.11	-2.43	-2.23
Ξ^{*0}	$\frac{2}{3}[\kappa_u - \kappa_s]$	0.64	-0.05	0.21
Ω^-	$-\kappa_s$	-1.83	-2.41	-2.02

TABLE III: Magnetic moments in nucleon magneton units $\mu_N = \frac{e}{2M_N}$, where M_N is the nucleon physical mass. Note that μ_{Ω^-} is not a prediction because it was used to fix κ_s .

parametrization for the isoscalar and isovector components inspired by vector meson dominance (VMD):

$$f_{1\pm} = \lambda + (1 - \lambda) \frac{m_v^2}{m_v^2 + Q^2} + c_\pm \frac{M_h^2 Q^2}{(M_h^2 + Q^2)^2}, \quad (24)$$

$$f_{2\pm} = \kappa_\pm \left\{ d_\pm \frac{m_v^2}{m_v^2 + Q^2} + (1 - d_\pm) \frac{M_h^2}{M_h^2 + Q^2} \right\}, \quad (25)$$

where m_v is the lightest vector meson mass fixed to $m_v = m_\rho$ (for $I = 1$) or m_ω (for $I = 0$), and c_\pm, d_\pm are VMD coefficients adjusted to fit the nucleon form factors. The model explicitly allows for the quarks to emerge as point-like particles at infinite Q^2 (as required by QCD) with an effective charge of λe_q . Fits to deep inelastic scattering (DIS) fixed $\lambda = 1.21$ (for our most efficient model II). The second term with the large mass M_h is intended to approximate the sum over contributions from heavy vector mesons, which characterize the short range structure of the VMD processes important at high Q^2 . We take M_h to be twice the nucleon mass ($M_h = 2M_N$) as in previous work [54, 55, 56, 57, 58, 59, 64].

We extend the model to the strange sector by defining the strange quark form factors:

$$f_{10} = \lambda + (1 - \lambda) \frac{m_\phi^2}{m_\phi^2 + Q^2} + c_0 \frac{M_h^2 Q^2}{(M_h^2 + Q^2)^2}, \quad (26)$$

$$f_{20} = \kappa_s \left\{ d_0 \frac{m_\phi^2}{m_\phi^2 + Q^2} + (1 - d_0) \frac{M_h^2}{M_h^2 + Q^2} \right\}. \quad (27)$$

This parametrization adds two more parameters to the model, (c_0, d_0), in addition to κ_s . Note that the ϕ meson is introduced to model the strange quark sector in the VMD framework. In this framework the dressed electromagnetic interaction (in the $t = q^2$ channel) is described as a succession of $u\bar{u}$ and $d\bar{d}$ pairs interacting to generate the ρ meson (for $I = 1$) or the ω meson (for $I = 0$), while for the strange quark sector this succession of $s\bar{s}$ interactions forms the ϕ meson.

The baryon scalar functions, ψ_B , that describe the momentum dependence of the quark-diquark system, are

parameterized in the following way:

$$\psi_{\Delta}(P, k) = \frac{N_{\Delta}}{m_D(\alpha_1 + \chi_{\Delta})^3} \quad (28)$$

$$\psi_{\Sigma^*}(P, k) = \frac{N_{\Sigma^*}}{m_D(\alpha_1 + \chi_{\Sigma})^2(\alpha_2 + \chi_{\Sigma})} \quad (29)$$

$$\psi_{\Xi^*}(P, k) = \frac{N_{\Xi^*}}{m_D(\alpha_1 + \chi_{\Xi})(\alpha_2 + \chi_{\Xi})^2} \quad (30)$$

$$\psi_{\Omega}(P, k) = \frac{N_{\Omega}}{m_D(\alpha_2 + \chi_{\Omega})^3}, \quad (31)$$

where

$$\begin{aligned} \chi_B &= \frac{(M_B - m_D)^2 - (P - k)^2}{m_D M_B} \\ &= \frac{2P \cdot k}{m_D M_B} - 2 \rightarrow 2 \left(\sqrt{1 + \frac{\mathbf{k}^2}{m_D^2}} - 1 \right) \\ &\simeq \frac{\mathbf{k}^2}{m_D^2} \quad \text{if } \mathbf{k}^2 \ll m_D^2, \end{aligned} \quad (32)$$

where the penultimate form holds in the rest frame of the baryon and shows that, in this frame, the argument χ_B is *independent* of the baryon mass. We will therefore choose the parameters α_1 and α_2 to also be independent of the baryon mass.

Since the momentum distribution is *defined* in the baryon rest frame, we see that the wave functions of all the baryons are spherically symmetric and that α_i defines the momentum ranges of the wave function in units of $k^2 \sim m_D^2$. For example, in the rest frame the Ω wave function is

$$\begin{aligned} \psi_{\Omega}(P, k) &= \frac{N_{\Omega}}{m_D \left(\alpha_2 + 2 \left(\sqrt{1 + \frac{\mathbf{k}^2}{m_D^2}} - 1 \right) \right)^3} \\ &\rightarrow \frac{N_{\Omega}}{m_D \left(\alpha_2 + \frac{\mathbf{k}^2}{m_D^2} \right)^3} \quad \text{if } \mathbf{k}^2 \ll m_D^2, \end{aligned} \quad (33)$$

showing that ψ_{Ω} behaves as a tripole at small $k = |\mathbf{k}|$, but only goes like k^{-3} at large k . However, when the bound state is moving in the z direction with large $\eta = P_z/M_B$, the wave function is distorted and no longer spherical. In a moving frame with $\eta \rightarrow \infty$, and ignoring all terms in the denominator of $\mathcal{O}(\eta^{-1})$,

$$\psi_{\Omega}(P, k) \rightarrow \frac{N_{\Omega}}{m_D \left(\alpha_2 - 2 + 2\eta \frac{k_-}{m_D} \right)^3} \quad (34)$$

where $k_- = E_D - k_z$ is the minus light-cone component of the diquark momentum. In coordinate space this wave function looks like a pancake.

With the inclusion of the factor $1/m_D$ in the wave function definition, the diquark mass dependence scales out of the integral Eq. (20), and the final result becomes independent of m_D [57]. We note that the parameter

α_1 is associated with the SU(2) sector (u and d quarks), while α_2 is associated with the s quark. A similar form to Eq. (28) was introduced in Ref. [54] to describe the dominant contribution of the $\gamma N \rightarrow \Delta$ transition in a model based only on the S-wave components, as in this study. (Originally the authors of Ref. [55] chose a wave function dependent on two range parameters, but later on concluded that one range parameter was enough, particularly at small Q^2 [56].)

As κ_s was fixed in the previous section by the value of μ_{Ω^-} , only c_0 , d_0 in Eqs. (27) and α_2 in the scalar functions $\psi_B(P, k)$ are not constrained. The remaining parameters are already fixed by the nucleon and Δ properties [55, 57]: the wave function parameter α_1 was fixed in Refs. [55]; the SU(2) current coefficients c_{\pm} , d_{\pm} were adjusted in Ref. [57]; $\lambda = 1.21$ from Ref. [57]. Because there is no experimental data for the electromagnetic form factors, except for Ω^- magnetic moment, we need to constrain the other parameters of our model using the recent lattice QCD data for the baryon decuplet [47]. In that work the Σ^{*+} , Σ^{*-} and Ξ^{*-} electromagnetic form factors were estimated using quenched lattice QCD at a momentum squared of $Q^2 = 0.230 \text{ GeV}^2$, for several values of m_{π} , in the range 300 MeV to 1 GeV [47]. The work also estimated the Δ electromagnetic form factors. However, because we want to use the same wave function parametrization for the Δ as in previous work [55, 56, 59], we do not use the Δ data in Ref. [47]. Study of the Δ electromagnetic form factors with the inclusion of the D-states can be found in Refs. [59, 61].

V. USING THE LATTICE DATA

To compare this model with lattice QCD data we follow the procedure presented in Refs. [56, 64]. Briefly, since lattice calculations are normally carried out for a variety of light quark masses larger than their physical values (as reflected in pion masses heavier than the physical pion, usually for m_{π} from about 300 MeV to about 1 GeV), we cannot compare our model to the lattice data unless we determine how our model will vary with the mass of the light quark.

To this end, we make the assumption that the range parameters in the baryon wave functions (α_1 and α_2) can be kept constant, but that the meson masses in the VDM description of the quark form factors ($m_v = m_{\rho}$, m_{ω} , or m_{ϕ} , and $M_h = 2M_N$) will vary with the actual values obtained in the lattice calculations. Furthermore, while the baryon wave functions do not depend on the baryon masses in their rest frame (justifying our assumption that the range parameters are also independent of the baryon masses), they do depend on the masses in the moving frames encountered when the form factors are calculated at nonzero Q^2 , and this is taken into account by using the lattice values of the baryon masses. The dependence on $m_{\rho} \simeq m_{\omega}$ in lattice calculations is parametrized by

the simple analytic form [65]

$$m_\rho = a_0 + a_2 m_\pi^2, \quad (35)$$

with $a_0 = 0.766$ GeV and $a_2 = 0.427$ GeV⁻¹, which are consistent with the available quenched lattice QCD data. As for the ϕ mass, the parametrization in lattice QCD requires some care. Different from the SU(2) sector, the realistic strange quark mass is currently used in lattice QCD calculations. In general, the properties of particles with strange quarks are used to fix the strange quark mass on the lattice. Although in dynamical simulations sea quarks contribute for the ϕ meson mass [48], in the quenched simulation the ϕ mass is independent of the light quark masses, thus independent of the pion mass. Because we apply our model to the quenched lattice QCD data determined at the physical strange quark mass [47], it may be justified to use the physical ϕ mass, $m_\phi = 1019$ MeV.

The above procedure assumes that the valence quark contributions are dominant, and that the quenched QCD data simulates well enough the valence quark effects. The sea quark degrees of freedom associated with intermediate meson states are not considered explicitly. In a formalism where the baryons are the effective degrees of freedom the virtual transitions between an initial baryon state and an intermediate baryon plus meson state can also contribute to the form factors. In that case the photon can also interact with the intermediate meson adding extra contributions to the form factors. According with χ PT the light meson gives the more important corrections. It is known however that in lattice QCD calculations the meson cloud effects are small in general for $m_\pi > 400$ MeV [66]. It is also known that quenched QCD underestimates the Δ^+ magnetic moment when the pion masses approaches to the physical point [67]. That effect was indeed observed in Refs. [45, 47]. However, the effects are not expected to be dominant in the lattice data analyzed in the present work² since the magnitude of the meson cloud becomes smaller when strange valence quarks are present.

In this work we use the form factor data in Ref. [47] and the lattice masses extracted for Σ^* and Ξ^* . For the nucleon we use the nucleon mass derived from the same group, with the same configuration in Ref. [68].³

To fix the strange quark mass in the quenched calculation, Ref. [47] chooses the symmetry point where the light quark mass equals the strange quark mass. At this point they find $m_K = m_\pi = 697$ MeV (and $m_\pi^2 = 0.485$

GeV²), which compares well with the experimental value of $2m_K^2 - m_\pi^2 = (0.693 \text{ GeV})^2$, a constraint on the strange quark mass motivated by leading order chiral perturbation theory.

VI. RESULTS

To determine the parameters c_0 , d_0 and α_2 we have minimized the χ^2 for the G_{E0} and G_{M1} form factor data in quenched lattice QCD from Ref. [47]. The data are composed of 12 values of m_π at one Q^2 ($Q^2 = 0.230$ GeV²), for Σ^{*+} , Σ^{*-} and Ξ^{*-} . The parameters c_0 , d_0 and α_2 are unconstrained, except for the condition $\alpha_2 > 0$. For κ_s we keep the value $\kappa_s = 1.462$ as determined by the physical Ω^- magnetic moment. The results are presented in Fig. 1. The values obtained from the fit, together with the other parameters, are presented in table IV.

The quality of the fit depends on the baryon considered. With the exclusion of the Ξ^{*-} data for G_{M1} , the fit is excellent for heavy pion masses; if we include G_{M1} for the Ξ^{*-} the fit is better for intermediate pion masses ($m_\pi = 690 - 830$ MeV). Because we are assuming that the momentum range parameters are independent of m_π , the failure of the model is expected for some high pion mass. As for the pion masses lower than 400 MeV, we can expect more deviation, since the effect of the pion cloud should become more important. In particular, for the magnetic dipole form factors it is known that the quenched data underestimate the valence quark contribution, as well as the result from full QCD (including meson cloud effects), particularly for the case of the Δ [47, 67]. For the Σ^* and Ξ^* , since the contribution of the light quarks (u or d) are smaller, the effect of the pion cloud is also expected to be smaller.

In Figs. 2 and 3 we show the electric charge G_{E0} and magnetic dipole G_{M1} form factors versus Q^2 , for Σ^{*+} , Σ^{*-} and Ξ^{*-} . We present results for the following three cases: $m_\pi = 697$ MeV corresponding to the SU(3) limit ($m_u = m_d = m_s$), the lightest pion ($m_\pi = 306$ MeV), and the physical point ($m_\pi = 138$ MeV), which corresponds to our prediction.

Figure 2 shows that a very good description is achieved for the electric form factor even for $m_\pi = 306$ MeV. As for the magnetic dipole form factor shown in Fig. 3, the deviation of the model from the quenched lattice QCD data is noticeable, particularly for the systems with two light quarks, (Σ^{*+} and Σ^{*-}). One can see that the model results are closer for Ξ^{*-} , particularly with the value, $m_\pi = 697$ MeV. We can interpret this deviation as a consequence of fact that the meson cloud effect included in the quenched data has the *wrong sign* (as has been observed for Δ^+ [47, 67]). For this reason it is natural to believe that the quenched data will not only underestimate the absolute value of the *exact* magnetic form factors, but also the valence contributions to the magnetic form factors included in our calculation.

Figure 4 compares the form factors of the different

² Considering the results of Ref. [47] for the Δ^+ magnetic moment, and the difference between the μ_{Δ^+} and the proton magnetic moment μ_p as a upper estimate of the pion cloud contribution, we conclude that these corrections are at most 30%.

³ For the pion mass $m_\pi^2 = 0.6920(35)$ GeV² there was no available M_N mass in Ref. [68], so we took the result for $m_\pi^2 = 0.6910(54)$ GeV². The difference between these m_π^2 values is smaller than the statistical error-bars.

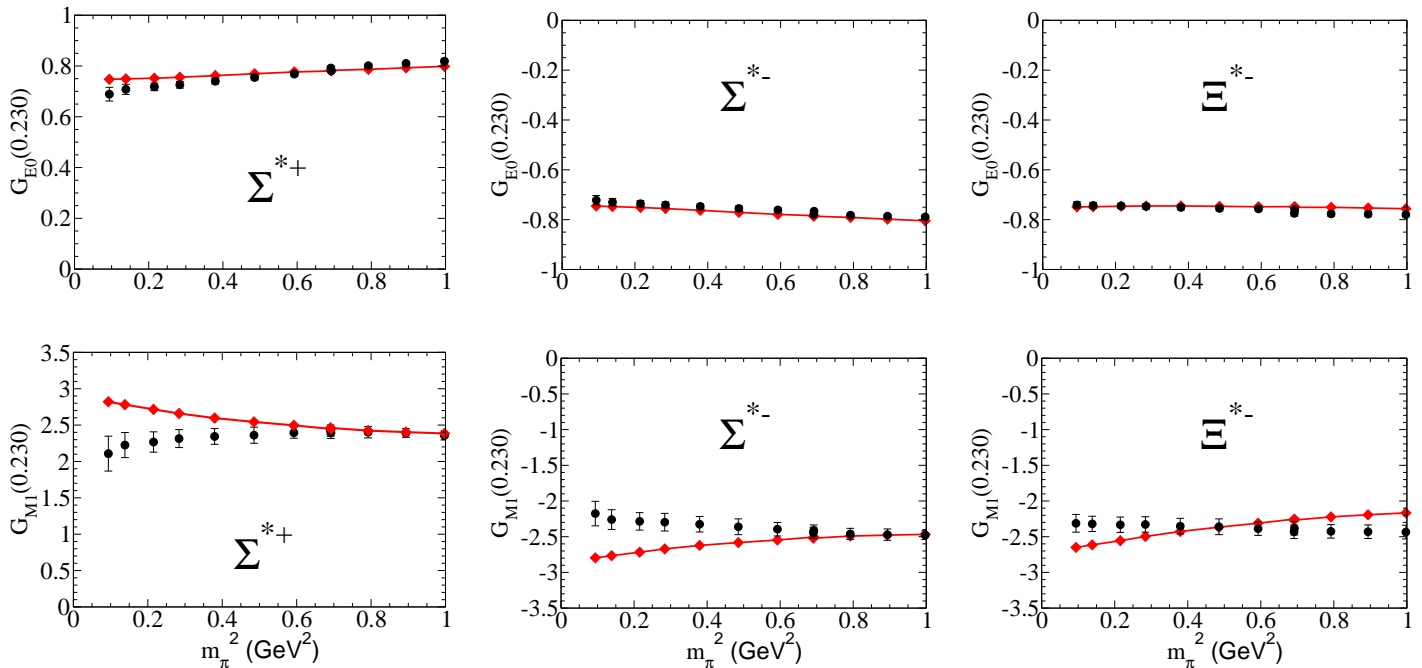


FIG. 1: Results of our fit to the lattice data from Ref. [47].

α_1, α_2	c_+, d_+	c_-, d_-	c_0, d_0	κ_u, κ_d	κ_s	N_Δ, N_{Σ^*}	N_{Ξ^*}, N_Ω
0.3366	4.160	1.160	4.427	1.777	1.462	2.594	0.901
0.1630	-0.686	-0.686	-1.860	1.915		1.553	0.510

TABLE IV: Results from the fit to the lattice QCD data. Only the variables in bold were adjusted in this work; the others were previously determined from fits to the nucleon form factors and $\gamma N \rightarrow \Delta$ transitions. The adjusted variables are: κ_s , fixed by the experimental result for μ_{Ω^-} [14]; c_0, d_0 , and α_2 , fixed by the fit to the lattice data [47] shown in Fig. 1. The normalization factors are a consequence of the values of α_1 and α_2 .

baryons with each other. We show our predictions for the absolute values $|G_{E0}|$ and $|G_{M1}|$ for Σ^{*+} , Σ^{*-} , and Ξ^{*-} at the physical point ($m_\pi=138$ MeV). The results for both form factors suggest very similar charge and magnetic moment distributions for the three baryons, even though the parametrization of the wave functions associated with the strange quark are substantially different (compare α_2 with α_1 in table IV). Another interesting point is that this similarity implies that SU(3) symmetry is approximately satisfied. Only the differences in masses of the baryons (Σ^* and Ξ^*) are responsible for the different values of $|\mu_B|$.

Once the parameters c_0, d_0 and α_2 are adjusted to the lattice QCD data, the Ω^- wave function at the physical Ω^- mass, and the quark current with the physical quark masses can be used to evaluate the Ω^- electromagnetic form factors. The results are presented in the table V and in the Fig. 5. At $Q^2 = 0$ the form factors are constrained by $e_{\Omega^-} = -1$ and by the experimental result for μ_{Ω^-} ,

but the evolution in Q^2 is a prediction.

Our results can be compared with the results in Ref. [47] for the Ω^- magnetic dipole form factor at $Q^2 = 0.230$ GeV², extracted from the simulation for the Δ^- at the pion mass $m_\pi = 697$ MeV: $G_{M1}(Q^2) = -2.36 \pm 0.11$. The experimental value (used in our calibration) which gives $G_{M1}(0) = \mu_{\Omega^-} \frac{M_\Omega}{M_N} = -3.60 \pm 0.10$ with μ_{Ω^-} in units μ_N [14], is also presented in the graph. In addition, there are unquenched lattice data at $Q^2 = 0$ from Aubin *et al.* [46]: $G_{M1}(0) = -3.44 \pm 0.14$, and the extrapolation from the Ref. [47] for $Q^2 = 0$: $G_{M1}(0) = -3.14 \pm 0.12$.

Finally, our model predicts the Ω^- squared radii of $\langle r_{E0}^2 \rangle = 0.22$ fm² and $\langle r_{M1}^2 \rangle = 0.27$ fm². These values are close to those estimated by the lattice QCD data in Ref. [47], which we have used to calibrate the s quark current and momentum distribution. In that work the corresponding results are: $\langle r_{E0}^2 \rangle = \langle r_{M1}^2 \rangle = 0.307 \pm 0.015$ fm². It is expected that inclusion of the meson cloud will increase that value [47]. Other estimates of

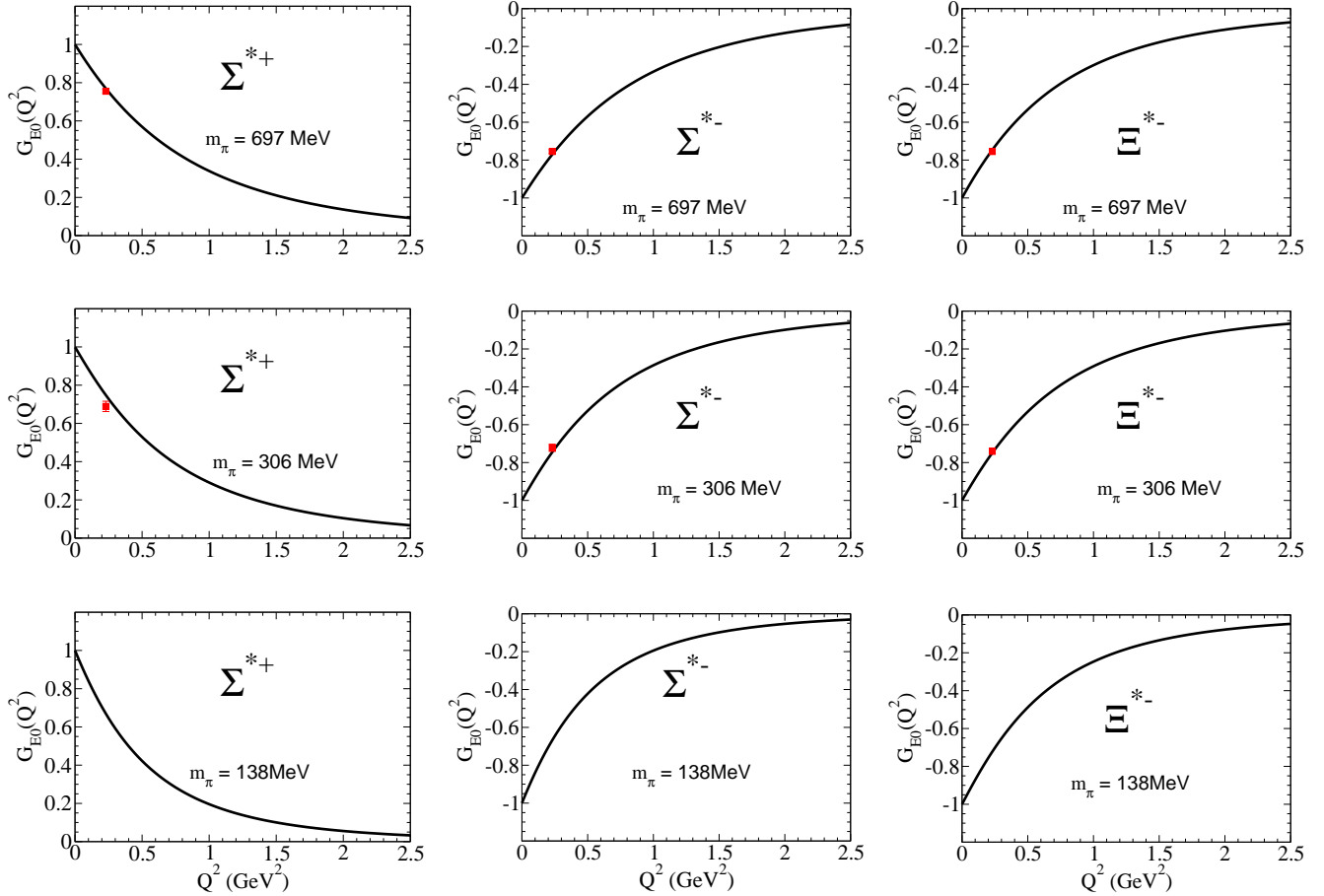


FIG. 2: G_{E0} form factors for Σ^{*+} , Σ^{*-} and Ξ^{*-} . The quenched lattice QCD data is from Ref. [47].

Q^2	$G_{E0}(Q^2)$	$G_{M1}(Q^2)$
0.00	-1.000	-3.604
0.25	-0.752	-2.635
0.50	-0.544	-1.862
0.75	-0.393	-1.322
1.00	-0.287	-0.954
1.25	-0.213	-0.700
1.50	-0.160	-0.524
1.75	-0.122	-0.399
2.00	-0.094	-0.308
2.25	-0.074	-0.242
2.50	-0.058	-0.192

TABLE V: Predictions for the Ω^- form factors.

the Ω^- charge radius [11, 15, 21, 22, 37, 39, 41] lead to a result between 0.16 fm^2 and 0.61 fm^2 , but not all the estimates are consistent with the experimental Ω^- magnetic moment. A chiral quark model with consistent exchange currents [22] that agrees with the data to a precision of

better than 6% predicts $\langle r_{E0}^2 \rangle = 0.61 \text{ fm}^2$.

VII. CONCLUSIONS

In this work we have extended the covariant spectator quark model (based on the Covariant Spectator Theory) to include the strange quark. We have chosen to study the baryon decuplet as a first application of the model because the structure (symmetric spin 3/2 state) is simpler than the baryon octet, where the spin 1/2 structure requires a mixture of diquark states with spin 0 and 1 [57]. Using the measured Ω^- magnetic moment and the recent lattice QCD data for the baryon decuplet [47] we have fixed the new model parameters associated with the s quark contributions to the current and the baryon wave functions.

The experimental result for μ_{Ω^-} fixes the anomalous magnetic moment of the strange quark, κ_s , at a value different from $\frac{1}{2}(\kappa_u + \kappa_d)$, suggesting a violation of the SU(3) symmetry at the level of 20%.

In this first study we have restricted the model to the description of the dominant form factors: G_{E0} and G_{M1} .

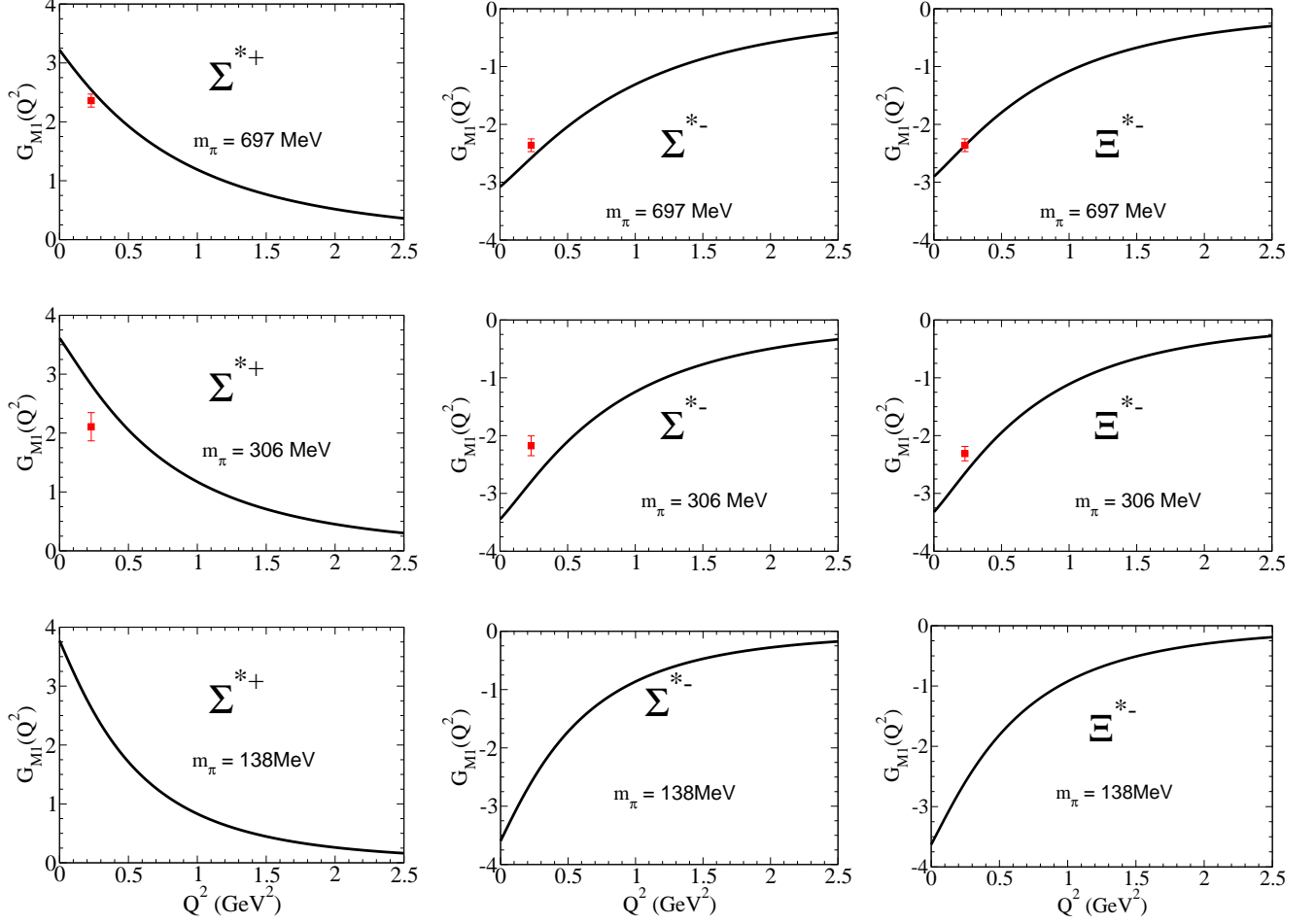


FIG. 3: G_{E0} form factors for Σ^{*+} , Σ^{*-} and Ξ^{*-} . The quenched lattice QCD data is from Ref. [47].

The subleading form factors G_{E2} and G_{M3} are also interesting for future study. For example, the subleading form factors can emerge in the present model when the D-states are included in the spin 3/2 systems. Although the D-states are important in the electromagnetic transition between the octet and the decuplet baryons (as an example for the $\gamma N \rightarrow \Delta$ transition), the D-states are not expected to be dominant for G_{E0} and G_{M1} , as was shown for the Δ case [58, 59, 61].

After calibration of the model, we have predicted the Ω^- form factors. The Ω^- is a very interesting object to study since it is composed of three strange quarks. Lattice QCD simulation for the Ω^- form factors can presently be performed at the physical strange quark mass [46, 47]. As the Ω^- is considerably more stable than the octet baryons and other members of the decuplet baryons except for the nucleons, there is a hope that the Ω^- form factors can be measured in the near future.

Our work so far is restricted to the valence quark degrees of freedom. This framework can be regarded as a good approximation since the meson cloud effects, the pion could as well as those of kaons, are expected to be

smaller, when strange quarks are present in the baryon. This statement is more valid for higher Q^2 and larger pion masses. The Ω^- meson cloud is expected to be small, although the difference between the extrapolation with the quenched lattice QCD data from Ref. [47] and the experimental result indicates that the meson cloud is not negligible. A possible reason for this is that the quenched calculations do not include the virtual transitions $\Omega^- \rightarrow \Xi K$ due to the omission of light quark loops (only the s quark is considered). Finally the discrepancy can also be partially due to the Ω^- mass, that in the quenched lattice simulation exceeds the physical mass by 3.6%. In future we plan to study these meson cloud effects.

We can also extend the present model to the study of the octet baryons, and to the heavy quark sector (c and b quarks), where valence quark degrees of freedom dominate.

Acknowledgments:

G. R. thanks David Richard, Huey-Wen Lin, Christopher Thomas and Nilmani Mathur for helpful discussions.

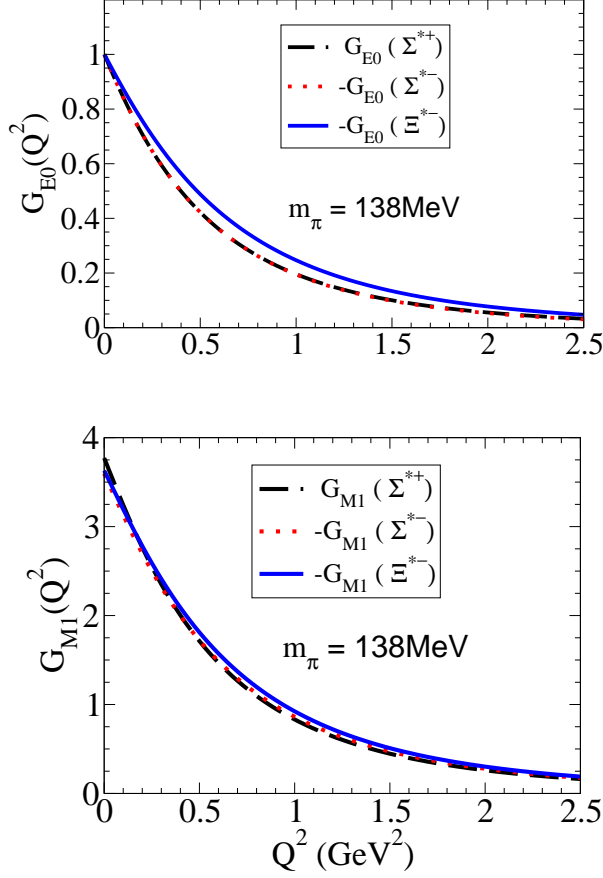


FIG. 4: Comparing G_α from Σ^{*+} with $-G_\alpha$ from Σ^{*-} and Ξ^{*-} .

This work was partially supported by Jefferson Science Associates, LLC under U.S. DOE Contract No. DE-AC05-06OR23177. G. R. was supported by the Portuguese Fundação para a Ciência e Tecnologia (FCT) under Grant No. SFRH/BPD/26886/2006. This work has been supported in part by the European Union (Hadron-Physics2 project “Study of strongly interacting matter”).

-
- [1] W. M. Yao *et al.* [Particle Data Group], J. Phys. G **33**, 1 (2006).
- [2] M. A. B. Beg, B. W. Lee and A. Pais, Phys. Rev. Lett. **13**, 514 (1964).
- [3] K. Hikasa *et al.* [Particle Data Group], Phys. Rev. D **45**, S1, (1992) (see p. 482); [Erratum-ibid. D **46**, 5210 (1992)].
- [4] Greiner Muller, **Quantum Mechanics Symmetries**, Springer-Verlag Berlin Heidelberg (1994).
- [5] T. Das and S. P. Misra, Phys. Lett. B **96**, 165 (1980).
- [6] Y. Tomozawa, Phys. Rev. D **25**, 795 (1982).
- [7] H. Georgi and A. Manohar, Phys. Lett. B **132**, 183 (1983).
- [8] R. C. Verma and M. P. Khanna, Phys. Lett. B **183**, 207 (1987).
- [9] M. I. Krivoruchenko, Sov. J. Nucl. Phys. **45**, 109 (1987) [Yad. Fiz. **45**, 169 (1987)].
- [10] J. H. Kim, C. H. Lee and H. K. Lee, Nucl. Phys. A **501** (1989) 835.
- [11] J. Kunz and P. J. Mulders, Phys. Lett. B **231**, 335 (1989); J. Kunz and P. J. Mulders, Phys. Rev. D **41**, 1578 (1990).
- [12] K. T. Chao, Phys. Rev. D **41**, 920 (1990).
- [13] H. T. Deihl *et al.* Phys. Rev. Lett. **67**, 804 (1991).
- [14] N. B. Wallace *et al.*, Phys. Rev. Lett. **74**, 3732 (1995).
- [15] B. Schwesinger and H. Weigel, Nucl. Phys. A **540**, 461 (1992).
- [16] S. T. Hong and G. E. Brown, Nucl. Phys. A **580**, 408 (1994).
- [17] P. Ha, Phys. Rev. D **58**, 113003 (1998) [arXiv:hep-ph/9804383].
- [18] J. Linde, T. Ohlsson and H. Snellman, Phys. Rev. D **57**, 5916 (1998) [arXiv:hep-ph/9709468].
- [19] S. L. Zhu, W. Y. P. Hwang and Z. S. P. Yang, Phys. Rev. D **57**, 1527 (1998) [arXiv:hep-ph/9802322].
- [20] F. Schlumpf, Phys. Rev. D **48**, 4478 (1993) [arXiv:hep-ph/9305293].
- [21] N. Barik, P. Das and A. R. Panda, Pramana **44** (1995) 145.
- [22] G. Wagner, A. J. Buchmann and A. Faessler, J. Phys. G **26**, 267 (2000).
- [23] T. M. Aliev, A. Ozpineci and M. Savci, Nucl. Phys. A **678**, 443 (2000) [arXiv:hep-ph/0002228].
- [24] A. Iqbal, M. Dey and J. Dey Phys. Lett. B **477**, 125 (2000) [arXiv:hep-ph/9906479].
- [25] B. O. Kerbikov and Yu. A. Simonov, Phys. Rev. D **62**, 093016 (2000) [arXiv:hep-ph/0001243].
- [26] J. Franklin, Phys. Rev. D **66**, 033010 (2002).
- [27] S. Sahu, Rev. Mex. Fis. **48**, 48 (2002).
- [28] C. S. An, Q. B. Li, D. O. Riska and B. S. Zou, Phys. Rev. C **74**, 055205 (2006) [Erratum-ibid. C **75**, 069901 (2006)].

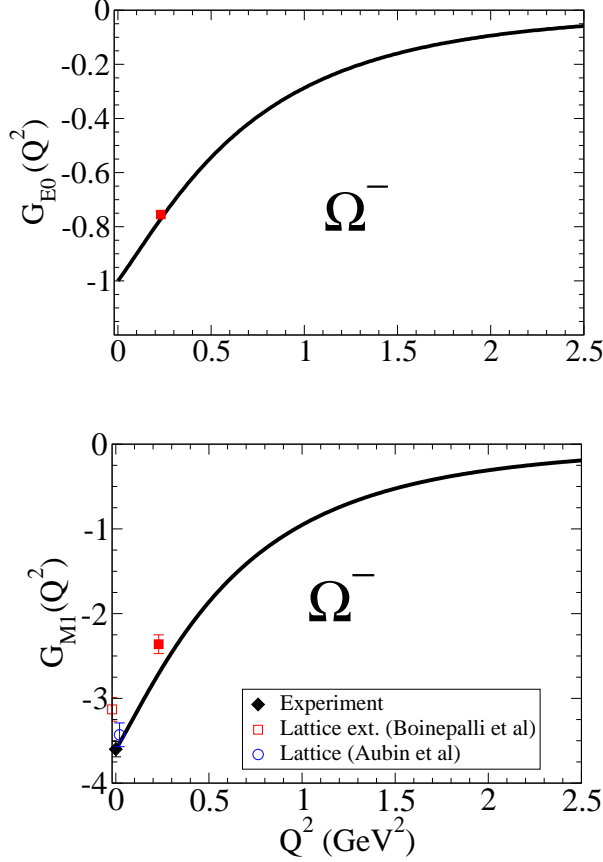


FIG. 5: Ω^- form factors. The squares represents the quenched lattice data from Ref. [47]. The circle represents the unquenched lattice data from Ref. [46].

- (2007) [arXiv:nucl-th/0610009].
- [29] T. Ledwig, A. Silva and M. Vanderhaeghen, Phys. Rev. D **79**, 094025 (2009) [arXiv:0811.3086 [hep-ph]].
- [30] T. M. Aliev, K. Azizi and M. Savci, arXiv:0904.2485 [hep-ph].
- [31] W. J. Leonard and W. J. Gerace, Phys. Rev. D **41**, 924 (1990).
- [32] S. S. Gershtein and Yu. M. Zinovev, Sov. J. Nucl. Phys. **33**, 772 (1981) [Yad. Fiz. **33**, 1442 (1981)].
- [33] J. M. Richard, Z. Phys. C **12**, 369 (1982).
- [34] N. Isgur, G. Karl and R. Koniuk, Phys. Rev. D **25**, 2394 (1982).
- [35] M. I. Krivoruchenko and M. M. Giannini, Phys. Rev. D **43**, 3763 (1991).
- [36] M. N. Butler, M. J. Savage and R. P. Springer, Phys. Rev. D **49**, 3459 (1994) [arXiv:hep-ph/9308317].
- [37] R. K. Sahoo, A. R. Panda and A. Nath, Phys. Rev. D **52**, 4099 (1995).
- [38] A. J. Buchmann and E. M. Henley, Phys. Rev. D **65**, 073017 (2002); A. J. Buchmann and R. F. Lebed, Phys. Rev. D **67**, 016002 (2003) [arXiv:hep-ph/0207358].
- [39] A. J. Buchmann, arXiv:0712.4383 [hep-ph].
- [40] L. S. Geng, J. Martin Camalich and M. J. Vicente Vacas, Phys. Rev. D **80**, 034027 (2009) [arXiv:0907.0631 [hep-ph]].
- [41] C. Gobbi, S. Boffi and D. O. Riska, Nucl. Phys. A **547**, 633 (1992).
- [42] A. J. Buchmann and E. M. Henley, Eur. Phys. J. A **35**, 267 (2008) [arXiv:0808.1165 [hep-ph]].
- [43] C. W. Bernard, T. Draper, K. Olynyk and M. Rushton, Phys. Rev. Lett. **49**, 1076 (1982).
- [44] D. B. Leinweber, T. Draper and R. M. Woloshyn, Phys. Rev. D **46**, 3067 (1992) [arXiv:hep-lat/9208025].
- [45] F. X. Lee, R. Kelly, L. Zhou and W. Wilcox, Phys. Lett. B **627**, 71 (2005) [arXiv:hep-lat/0509067].
- [46] C. Aubin, K. Orginos, V. Pascalutsa and M. Vanderhaeghen, Phys. Rev. D **79**, 051502(R) (2009) [arXiv:0811.2440 [hep-lat]].
- [47] S. Boinepalli, D. B. Leinweber, P. J. Moran, A. G. Williams, J. M. Zanotti and J. B. Zhang, arXiv:0902.4046 [hep-lat].
- [48] H. W. Lin *et al.* [Hadron Spectrum Collaboration], Phys. Rev. D **79**, 034502 (2009) [arXiv:0810.3588 [hep-lat]].
- [49] B. C. Tiburzi and A. Walker-Loud, Phys. Lett. B **669**, 246 (2008). [arXiv:0808.0482 [nucl-th]].
- [50] S. Aoki *et al.* [PACS-CS Collaboration and PACS-CS Collaboration and PACS-CS Collaboration], Phys. Rev. D **79**, 034503 (2009) [arXiv:0905.0962 [hep-lat]].
- [51] V. Drach *et al.*, PoS **LATTICE2008**, 123 (2008) [arXiv:0905.2894 [hep-lat]].
- [52] F. Gross, Phys. Rev. **186**, 1448 (1969); F. Gross, J. W. Van Orden and K. Holinde, Phys. Rev. C **45**, 2094 (1992).
- [53] F. Gross, G. Ramalho and M. T. Peña, Phys. Rev. C **77**, 035203 (2008).
- [54] G. Ramalho, M. T. Peña and F. Gross, Eur. Phys. J. A **36**, 329 (2008) [arXiv:0803.3034 [hep-ph]].
- [55] G. Ramalho, M. T. Peña and F. Gross, Phys. Rev. D **78**, 114017 (2008) [arXiv:0810.4126 [hep-ph]].
- [56] G. Ramalho and M. T. Peña, Phys. Rev. D **80**, 013008 (2009) [arXiv:0901.4310 [hep-ph]].
- [57] F. Gross, G. Ramalho and M. T. Peña, Phys. Rev. C **77**, 015202 (2008) [arXiv:nucl-th/0606029].
- [58] G. Ramalho and M. T. Peña, J. Phys. G **56**, 0805004 (2009) [arXiv:0807.2922 [hep-ph]].
- [59] G. Ramalho, M. T. Peña and F. Gross, Phys. Lett. B **678**, 355 (2009) [arXiv:0902.4212 [hep-ph]].
- [60] F. Gross and P. Agbakpe, Phys. Rev. C **73**, 015203 (2006) [arXiv:nucl-th/0411090].
- [61] G. Ramalho, Franz Gross and M. T. Peña, *Electromagnetic form factors of the Delta in a D-wave approach*, work in preparation
- [62] S. Nozawa and D. B. Leinweber, Phys. Rev. D **42**, 3567 (1990).
- [63] V. Pascalutsa, M. Vanderhaeghen and S. N. Yang, Phys. Rept. **437**, 125 (2007) [arXiv:hep-ph/0609004].
- [64] G. Ramalho and M. T. Peña, arXiv:0812.0187 [hep-ph], to appear in J. Phys. G.
- [65] D. B. Leinweber, A. W. Thomas, K. Tsushima and S. V. Wright, Phys. Rev. D **64**, 094502 (2001) [arXiv:hep-lat/0104013].
- [66] W. Detmold, D. B. Leinweber, W. Melnitchouk, A. W. Thomas and S. V. Wright, Pramana **57**, 251 (2001) [arXiv:nucl-th/0104043]; J. D. Ashley, D. B. Leinweber, A. W. Thomas and R. D. Young, Eur. Phys. J. A **19**, 9 (2004) [arXiv:hep-lat/0308024].
- [67] R. D. Young, D. B. Leinweber and A. W. Thomas, Nucl. Phys. Proc. Suppl. **128**, 227 (2004) [arXiv:hep-lat/0311038]; D. B. Leinweber,

A. W. Thomas, A. G. Williams, R. D. Young, J. M. Zanotti and J. B. Zhang, Nucl. Phys. A **737**, 177 (2004) [arXiv:nucl-th/0308083].

[68] S. Boinepalli, D. B. Leinweber, A. G. Williams,

J. M. Zanotti and J. B. Zhang, Phys. Rev. D **74**, 093005 (2006) [arXiv:hep-lat/0604022].